Rejection of Perfluoroalkyl Acids by Nanofiltration and Reverse Osmosis in a High-Recovery Closed-Circuit Membrane Filtration System

Safulko, A.^{1,2}, Cath, T.Y.¹, Li, F.¹, Tajdini, B.¹, Boyd, M.³, Huehmer, R.P.³, Bellona, C.^{1*}

¹Department of Civil and Environmental Engineering, Colorado School of Mines, Golden, CO 80401, USA

²Brown and Caldwell, Lakewood, CO 80401, USA

³Desalitech Inc, Marlborough, MA 01752, USA

* Corresponding author: cbellona@mines.edu

In preparation for submission to: Separation and Purification Technology

Abstract

Poly- and perfluoroalkyl substances (PFASs), especially perfluoroalkyl acids (PFAAs), have garnered broad attention due to their near ubiquitous presence in environmental and biological matrices, recalcitrant nature, and reported negative human health impacts. Processes using highpressure membranes such as reverse osmosis (RO) and nanofiltration (NF) have been investigated as PFAA treatment technologies due to their ability to separate dissolved solutes such as inorganic ions, and small molecular weight organic compounds. The major drawback associated with high-pressure membranes is management of the concentrate stream produced during treatment. As a result, high recovery membrane system configurations have been developed with the goal of minimizing volume of concentrate requiring disposal. In the context of PFAS treatment, high-recovery membrane applications may be beneficial; PFAS residuals could be concentrated allowing advantages in terms of disposal, e.g., more effective application of PFAS destruction technologies. The objective of this study was to evaluate the PFAA rejection performance of commercially available high-pressure membranes in a pilot-scale closed-circuit membrane filtration (CCMF) system. The rejection of nine PFAAs by four spiral wound membrane products spanning characteristics ranging from loose NF to seawater RO was investigated during and through two closed-circuit sequences each operating up to 97% recovery. Mechanisms of PFAA rejection including steric and electrostatic exclusion were investigated through analysis of generated data, and ionic strength experiments. Additionally, short-term foulant accumulation during CCMF and normalized energy analysis were performed by monitoring the calculated temperature corrected specific flux (TCSF) and design software simulations, respectively. Results from this study demonstrate that tight NF and RO membranes are effective for separating and concentrating PFAAs during high recovery CCMF operation. During CCMF sequences to 97% water recovery, the NF90, CR100, and SW30 membranes evaluated exhibited overall rejection values of >98.3% for the PFAAs quantified in this study. The loose NF membrane element investigated (NF270) exhibited the lowest PFAA rejection performance during the high recovery experiments, particularly at water recoveries >90%. Diminished PFAA rejection performance of the NF270 is likely a result of both steric and electrostatic exclusion being significant separation mechanisms. Feed water amended with sodium sulfate yielded lower rejection for PFAAs by the NF270 compared to unamended feed water supporting the hypothesis that that high recovery CCMF operation may negatively impact PFAS rejection by loose NF membranes, particularly membranes that rely on electrostatic exclusion for separation of anions.

Keywords: PFAS, Perfluoroalkyl acids, reverse osmosis, nanofiltration, high-pressure membranes

1. Introduction

Per- and polyfluoroalkyl substances (PFAS) are a large group of fluorine containing compounds used in a variety of applications [1]. PFAS, and in particular perfluoroalkyl acids (PFAAs), have garnered broad attention due to their near-ubiquitous presence in environmental and biological matrices, recalcitrant nature, and reported negative human health impacts [1-4]. As a result, several countries have developed screening levels or regulatory standards for certain PFAAs, with the USEPA recently lowering health advisory levels for perfluorooctanoic acid (PFOA) and perfluorooctanoic sulfonate (PFOS) to sub-ng/L levels [5-7]. In early 2023, the USEPA released a proposed PFAS national primary drinking water regulation with maximum contaminant limits for PFOA and PFOS at 4 ng/L each, and a hazard index approach for four additional PFAS [8]. Numerous studies have highlighted challenges associated with the treatment of PFAAs as they are mostly resistant to oxidation processes (e.g., ozone, hydroxyl radicals) and not effectively removed by conventional water treatment processes [9-11]. Several notable destruction technologies relying on reductive processes and chemical or thermal decomposition have been developed, although these processes reportedly require substantial energy inputs for log reductions of PFAS, especially short-chain PFAAs [12-17]. As a result, the current best available treatment approach for the removal of PFAAs is adsorption, primarily using granular activated carbon (GAC) and/or anion exchange resin (AER) [10, 18-20]. Reported drawbacks of adsorbent treatment include rapid breakthrough of certain PFAAs and frequent changeouts, decreased performance due to competitive adsorbates, and disposal of spent adsorbents [9, 10, 18, 20].

Reverse osmosis (RO) and nanofiltration (NF) have been identified as viable PFAS treatment technologies due to their ability to separate dissolved ions and low molecular weight organic compounds from water [21-23]. Electrostatic and size exclusion of anionic PFAAs by RO and NF membrane polymers is believed to lead to effective separation, and past studies have reported greater than 90% rejection of various PFAAs [22-24]. For example, Appleman et al. [24] evaluated the separation performance of nine perfluoroalkyl acids (PFAAs) by a loose NF

(NF270) membrane across three synthetic water matrices and a range of flux conditions (17 to 75 LMH) and reported target PFAA rejection >95% except for perfluorobutanoic acid (PFBA; ~93%). It is worth noting that these past studies were performed using small bench-scale membrane systems that may not represent conditions consistent with full-scale membrane systems. Additionally, reported high PFAA rejection values are often calculated using very low permeate concentrations or using detection limits due to non-detects in permeate samples [22, 24].

System conditions such as permeate flux and recovery, membrane fouling, and background water matrix constituents can reportedly influence the rejection of PFAS by NF and RO membranes [22, 23, 25-27]. Mechanisms influencing the separation of solutes by NF and RO membranes has been the focal point of numerous studies [28-30] and include solute and membrane properties, system operating conditions, and feed water quality. Solute properties believed to dictate separation efficiency include molecular size, charge, and adsorbability (e.g., hydrophobic interactions, hydrogen bonding) [31-36]. PFAA's low pKa values render them anionic at near-neutral pH and their molecular weights are generally near to or greater than molecular weight cut-offs (MWCO) of RO and most NF membranes. However, several recent studies have reported that the unique properties of PFAAs, in particular their hydrophobicity and relatively low critical micelle concentration, may impact separation performance in certain scenarios [27, 37, 38]. For example, Wang et al. [27] reported increased PFOS and perfluorobutanoic sulfonate (PFBS) rejection with increasing feed water concentration, decreased rejection with increasing ionic strength (PFBS), and that adsorptive effects influenced separation (mainly PFOS). Liu et al. [23] reported substantially lower PFAA rejection by the NF270 membrane (FilmTecTM) when performing experiments on contaminated groundwater compared to deionized water amended with PFAAs, highlighting the potential influence of ionic strength on rejection.

One major drawback associated with high-pressure membranes is management of the retentate stream produced during treatment, which has frequently been cited as the most divisive issue preventing widespread adoption of NF and RO membrane processes [39, 40]. Within the last decade, closed-circuit membrane filtration (CCMF) has emerged as a promising high-recovery membrane process [41-43] that uses recirculation of retentate to decouple flux, recovery, and crossflow velocity during operation. Compared to single-pass high-pressure

membrane systems, a CCMF system can achieve comparably high recovery in a substantially reduced footprint, with a lower specific energy requirement, and increased operating flexibility [44-46]. A recent study by Warsinger et al. [47] suggests that the operational transience that comprises the semi-batch CCMF operation is a major factor in reducing the potential for inorganic fouling, even when foulants are concentrated beyond theoretical saturation limits [45]. Considering the potential for substantial volumetric recovery improvement, energy/cost savings, and increased operational flexibility, the CCMF approach is a feasible alternative to conventional high pressure membrane systems. In the context of PFAS treatment, high-recovery membrane applications may be beneficial because PFAS residuals could be concentrated, allowing advantages in terms of disposal and more effective application of PFAS destruction technologies. Several recent studies have evaluated a treatment train approach consisting of RO or NF preceding brine-based treatment [48].

Because most studies on PFAA rejection by NF/RO have been performed at bench-scale using model water solutions, there is a need to evaluate PFAA rejection at larger scales with realistic water matrices and operating conditions. The objective of this study was to evaluate the PFAA rejection performance of commercially available high-pressure membranes spanning characteristics of loose NF to tight RO in a pilot-scale CCMF system operating at up to 97% recovery treating dechlorinated tap water spiked with PFAAs. Evaluation of PFAA rejection during CCMF operation is advantageous as it allowed simultaneous investigation of the impact of recovery (i.e., PFAA concentration) and water matrix (i.e., ionic strength) on PFAA separation, and quantification of rejection at levels greater than 99 percent. Mechanisms of PFAA rejection including steric and electrostatic exclusion were investigated through analysis of generated data, and ionic strength experiments. Additionally, short-term foulant accumulation during CCMF and normalized energy analysis were performed by monitoring the calculated temperature-corrected specific flux (TCSF) and design software simulations, respectively.

2. Materials and methods

2.1. CCMF pilot system

A DesaliTecTM CCMF pilot system provided by Desalitech Inc (Marlborough, MA) was used for membrane evaluation experiments (Figure 1). The pilot system was housed in a 32-foot shipping container and contained a single, four membrane long pressure vessel configured to

hold three 8-inch by 40-inch spiral wound membrane elements and one membrane spacer. The pilot system has an automated, integrated programmable logic controller (PLC) that controls pumps speed, scale-inhibitor dosing rate, volumetric recovery, and permeate flux. Sensors installed in the system included flow meters, pressure transmitters, thermocouples, pH, and conductivity probes. During closed-circuit operation, retentate and associated solutes retained by the membrane were recirculated to provide a constant crossflow rate using a recirculation pump. Once the defined recovery was achieved, the system was flushed under plug-flow conditions until the dead volume of the feed-side portion of the system had been flushed through the retentate discharge valve. Once the retentate had been purged from the system, the retentate discharge valve was closed and closed-circuit operation resumed.

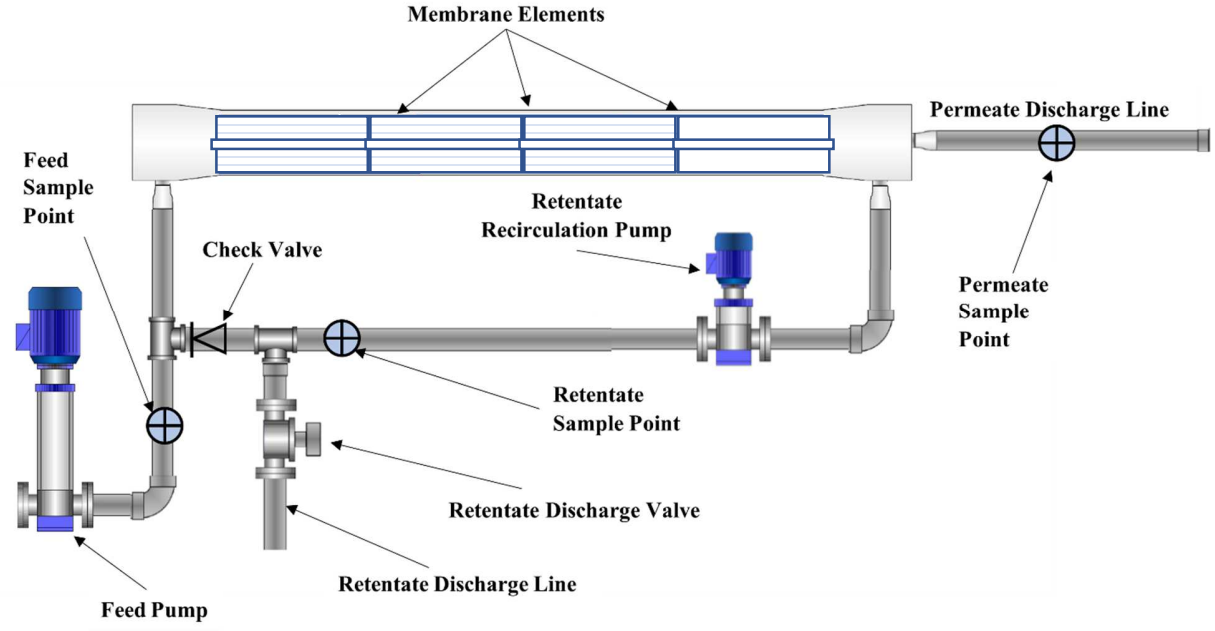


Figure 1. A flow diagram of the pilot CCMF system. A single, four membrane long pressure vessel was configured to hold three 8-inch by 40-inch spiral wound membrane elements and one membrane spacer. High pressure feed pump delivers makeup water to the system at a flowrate similar to the permeate flowrate. A brine recirculation pump maintains cross flow velocity through the membrane elements.

2.2. PFAAs evaluated

PFAAs were introduced into the feed water used in membrane experiments through dosing of an aqueous film-forming foam (AFFF) concentrate solution. Using a targeted PFAS analytical (section 2.5) method, the fate of nine PFAAs was tracked during membrane experiments (Table

1). The PFAAs evaluated spanned a range of chain lengths (C3 - C8) and were comprised of both perfluoroalkyl-carboxylic and -sulfonic acids. Relevant characteristics of evaluated PFAAs are presented in Table 1.

Table 1. Physio-chemical characteristics of nine studied PFAAs including names, abbreviations, number of carbon atoms, bulk diffusivity $(D)^{\alpha}$, octanol-water partition coefficient $(\log Kow)^{\beta}$, molecular weight, acid dissociation constant $(pKa)^{\beta}$.

PFAA Compound, number of carbons	Category	Bulk diffusivity (D) [cm²/sec]	Log K _{ow}	Log D _{OW} [pH 7]	MW [g/mol]	pK _a
Perfluoropentanoic acid (PFPeA), C5	Carboxylic, short chain	7.19×10^{-6}	2.37	-0.52	264.0	0.34
Perfluorohexanoic acid (PFHxA), C6	Carboxylic, short chain	6.58×10^{-6}	3.20	0.18	314.1	0.32
Perfluorooctanoic acid (PFOA), C8	Carboxylic, long chain	5.63×10^{-6}	5.23	1.58	414.1	0.3
Perfluoropropanesulfonic ac (PFPrS), C3	Sulfonic, short chain	7.91×10^{-6}	1.40	-0.45	250.1	3.31
Perfluorobutanesulfonic acid (PFBS), C4	Sulfonic, short chain	7.15×	2.05	0.25	300.1	3.31
Perfluoropentanesulfonic acid (PFPeS), C5	Sulfonic, short chain	6.52×10^{-6}	2.96	0.95	350.1	3.32
Perfluorohexanesulfonic aci (PFHxS), C6	Sulfonic, short chain	6.01×10^{-6}	3.96	1.65	400.1	3.32
perfluoroheptanesulfonic acid (PFHpS), C7	Sulfonic, long chain	5.58×10^{-6}	5.06	2.35	472.1	3.32
Perfluorooctanesulfonic acid (PFOS), C8	Sulfonic, long chain	5.21×10^{-6}	5.50	3.05	500.1	3.32

α Estimated values using SPARC (ARChem, http://www.archemcalc.com/).

2.3. Membranes

Four commercial, high-pressure membranes were selected for PFAA rejection experiments operating under high recovery conditions in the CCMF pilot system. Virgin 8040 (8-inch diameter x 40-inch length) spiral wound membrane elements were utilized. The membrane

β Estimated data adapted from Marvin Sketch 22.2 (ChemAxon Ltd., http://www.chemaxon.com/).

products selected included the FilmTecTM NF270 (loose NF), FilmTecTM NF90 (tight NF), FilmTecTM CR100 (RO), and FilmTecTM SW30 (SWRO) (FilmTecTM, Edina, MN). The selected membranes were chosen based on their characteristic separation performance spanning loose NF to tight RO. Table 2 summarizes select properties and characteristics of the membrane evaluated during this study.

Table 2. Summary of membrane characteristics

Parameter	NF270-400/34i	NF90- 400/34i	CR100- 400	SW30XFR- 400/34
Classification	NF	NF	RO	RO
Manufacturer	FilmTec TM	FilmTec TM	FilmTec TM	FilmTec TM
Active layer	Semi-aromatic	Aromatic	Aromatic	Aromatic
	polyamide	polyamide	polyamide	polyamide
Isoelectric point	$2.56^{a}, <3^{b}$	$3.43^{a}, <4^{b}$	<3	<3
Zeta potential (mV) at pH=6 ¹	-146 ¹	-96 ¹	-78 ¹	-100^{1}
Average pore radius (nm)	$0.42^{\rm d}$, $0.41^{\rm d}$, $0.44^{\rm f}$	$0.34^{\rm d}, 0.38^{\rm f}$	-	-
MWCO (g/mol)	$340^{\rm f}, 200^{\rm g}$	180 ^f , 200 ^h	-	<100
Pure water permeability (LMH/bar)	$14.0^{i}, 17.1^{j}$	11.44 ^j	-	1.6^{k}
Membrane active area (ft²/element)	400^{1}	400^{1}	400	400^{1}

a. [49], b. [50], c. [51], d. [52], e. [53], f. [54], g. [55], h. [56], i. [57], j. [58], k. [59], l. Information supplied by manufacturer.

2.4. PFAA rejection experiments

Prior to rejection experiments, membrane integrity was first evaluated by operating the system with dechlorinated tap water under operating parameters similar to the manufacturer's specification. A summary of the membrane break-in operating condition is provided in Table S.1, and operating conditions during experiments are summarized in Table 3. Following validation of membrane break-in and integrity, high recovery PFAA rejection experiments were initiated. During all experiments feed flow rate was constant at 10 gpm (37.9 LPM) with feed pressure modulated to maintain a constant flux of 12 gfd (20 LMH). Generated permeate was continuously discharged to a 2,000-gallon tank. The retentate recirculation flow rate was set at 25 gpm during all experiments. Membrane experiments were conducted over two sequences where each sequence is defined by the period of CCMF operation followed by the plug flow flush.

Table 3. Operating conditions for the experiments

Parameter	Value
Feed flow, Q_f (gpm (LPM))	10 (37.9)

Retentate recirculation flow, Q _r (gpm (LPM))	25 (94.6)
Permeate flow, Q _p (gpm (LPM))	10 (37.9)
Flux (gfd (LMH))	12 (20)
Target recovery (%)	97
Scale-inhibitor dose (mg/L)	1.6

For each membrane experiment, a batch (1,700-gallons) of feed water was prepared using dechlorinated tap water (3 mg/L of granular anhydrous sodium metabisulfite added (Spectrum Chemical, New Brunswick, NJ)). The feed water pH was adjusted to 6.3 with 93.4% sulfuric acid (Chemtrade, Toronto, ON). Following dichlorination and pH adjustment, the feed water was spiked with a PFAA AFFF concentrate solution to achieve a nominal PFOS concentration of 15,000 ng/L. Prior to beginning each experiment, the feed water was mixed well for a minimum of 1 hour. Feed water quality parameters for the NF270, NF90, CR100, and SW30 experiments are summarized in Table 4. During each experiment, an inline chemical dosing pump dosed a proprietary scale-inhibitor (American Water Chemicals, Plant City, FL) solution to a target dose of 1.6 mg/L.

Table 4. Average general feed water quality for water used in the rejection experiments. Scale-inhibitor and PFAAs were added to the water before each experiment.

Parameter	Unit	Average	Std Dev	
		(n=8)		
pН	-	8.5	0.07	
Alkalinity	mg/L as CaCO ₃	57	7	
TOC	mg/L	2.96	0.74	
Fluoride	mg/L	0.65	0.14	
Chloride	mg/L	24.01	3.21	
Sulfate	mg/L	88.23	13.72	
Barium	mg/L	0.044	0.005	
Calcium	mg/L	25.80	8.66	
Potassium	mg/L	2.15	1.46	
Magnesium	mg/L	5.64	1.24	
Sodium	mg/L	20.40	2.64	

For each experiment, three feed water samples were collected for PFAA analysis (see section 2.5) from the pressurized feed line during each sequence, totaling six feed water PFAA samples per experiment. Concentrations of selected PFAAs measured by targeted analysis in AFFF spiked feed water for the NF270 experiment are summarized in Table 5. The feed water PFAA characterization for the NF90, CR100, and SW30 experiments are summarized in Tables S.2, S.3, and S.4. In addition, for each high-recovery CCMF membrane experiment sequence,

permeate and retentate samples were collected at various recovery monitoring points (75%, 80%, 85%, 90%, 92%, 94%, 95%, 96%, and 97%). Permeate generated during each CCMF membrane experiment was collected in a 2,500-gallon HDPE tank and subsequently sampled for PFAA analysis (termed permeate tank sample). Given the large volume of the permeate tank and potential for cross-contamination between membrane experiments, an additional method of estimating combined permeate concentrations by using PFAA permeate concentrations measured at discrete recovery values was employed. A description of the employed Riemann model approach to estimate permeate tank PFAA concentrations is provided in the SI.

Table 5. Measured NF270 PFAA feed water concentrations and limits of quantification (LOQ) for sample types collected

		PFAS Analyte (n=6)								
		PFPeA	PFHxA	PFOA	PFPrS	PFBS	PFPeS	PFHxS	PFHpS	PFOS
Avg	feed	191	579	373	326	696	1056	3393	123	15311
(ng/L)										
Std. Dev.		33	72	131	15	140	113	178	53	2327
RSD (%)		17.1	12.4	35.2	4.5	20.2	10.7	5.2	43.2	15.2
Permeate	LOQ ^a	1	1	5	1	20	1	1	2	10
Feed LO	Q^a	10	10	50	10	200	10	10	20	100
Retentate	LOQ ^a	100	100	500	100	2000	100	100	200	1000

a. LOQ presented in ng/L units and vary due to sample dilutions.

PFAA rejection was assessed using two methods termed in this study as observed and intrinsic rejection using Eqns. 1 and 2, respectively:

$$R_{obs} = 1 - \left(\frac{C_{p,i}}{\overline{C_f}}\right) \tag{1}$$

$$R_{int} = 1 - \left(\frac{C_{perm,i}}{\left[\left(\overline{C_f} * 0.2857 \right) + \left(C_{r,i} * 0.7143 \right) \right]} \right)$$
 (2)

where R_{obs} is the observed rejection, R_{int} is the intrinsic rejection, i is the recovery setpoint, $C_{p,i}$ is the solute permeate concentration at recovery i, $\overline{C_f}$ is the average feed concentration of the solute, and $C_{r,i}$ is the solute retentate concentration at recovery i. Because the flux and retentate recirculation rate were held constant, the feed and retentate weighting coefficient in Equation 2

b. RSD is the relative standard deviation calculated from 6 samples

were fixed during CCMF operation and calculated based on the 10 gpm of feed flow and 25 gpm of retentate recirculation flow entering the leading side of the pressure vessel.

2.5. Water analysis

Samples were collected for analysis in 15 mL polypropylene centrifuge tubes (Falcon; Corning, NY). Samples were analyzed for targeted PFAA using liquid chromatography quadrupole time-of-flight mass spectrometry (LC-QToF-MS). PFAAs were measured on a SCIEX X500R QTOF-MS system (Framingham, MA) using electrospray ionization in negative mode (ESI-) with SWATH® Data-Independent Acquisition for both TOFMS and MS/MS mode. Target analytes were identified based on retention time and mass compared to analytical standards, and quantified using calibration standards ranging from 0.074 ng/L to 7.4 μ g/L, with most analytes having a minimum limit of quantitation (LOQ) between 0.074 ng/L and 7.4 ng/L. The analytical column used was a Phenomenex (Torrance, CA) Gemini C18, 5 μ m, 100 mm x 3 mm.

Additional water quality parameters analyzed included total organic carbon (TOC), anions, cations, and metals. TOC was measured using a carbon analyzer (Shimadzu ion TOC-L, Columbia, MD). Anions were measured using ion chromatography (IC; ICS-900, Dionex, Sunnyvale, CA), while cations/metals were analyzed using inductively coupled plasma optical emission spectroscopy (ICPOES; optima 5300 DV, PerkinElmer, Fremont, CA).

3. Results and discussion

3.1. Comparative analysis of candidate membranes

Candidate membranes were evaluated over two closed-circuit sequences (up to 97% recovery for each) during which samples were collected for PFAA analysis and operating data collected through the system PLC. The following sections detail comparison between the membranes evaluated.

3.1.1. Operating performance

Membrane permeability and fouling was evaluated by calculating the temperature corrected specific flux (TCSF) as a function of recovery (up to 97%) during each two-sequence experiment (Figure 2). The selected NF membranes (NF270 and NF90) exhibited higher average TCSF

relative to the selected RO membranes (CR100 and SW30) due to substantially higher permeability. The NF270 and SW30 membranes did not experience measurable fouling during the two-sequence experiment as evidenced by the relatively stable TCSF. Alternatively, the NF90 and CR100 exhibited evidence of fouling during both CCMF sequences and CR100 exhibited a 15.2% and 12.7% decrease in TCSF during each CCMF sequence, respectively. However, the observed fouling of the NF90 and CR100 membranes was reversed by the intervening plug flow flush, with each membrane recovering to baseline TCSF conditions between sequences. Given the short duration of the experiments in this study, the effect of long term, high-recovery operation, with respect to fouling, on the membranes tested remains unknown and a topic for future investigation. Utilizing the operating conditions and feed water quality presented in Tables 3 and 4, respectively, the specific energy for each membrane experiment was estimated with the WAVETM modeling software (FilmTecTM, Edina, MN) and is presented in kilowatt hours per cubic meter (kWh/m³) in Table 6. As anticipated, specific energy increases as a function of membrane selectivity, increasing from loose NF to tight RO. Similarly, the rejection of conductivity and major cations and anions generally increased when going from loose NF to tight RO (Table S.5).

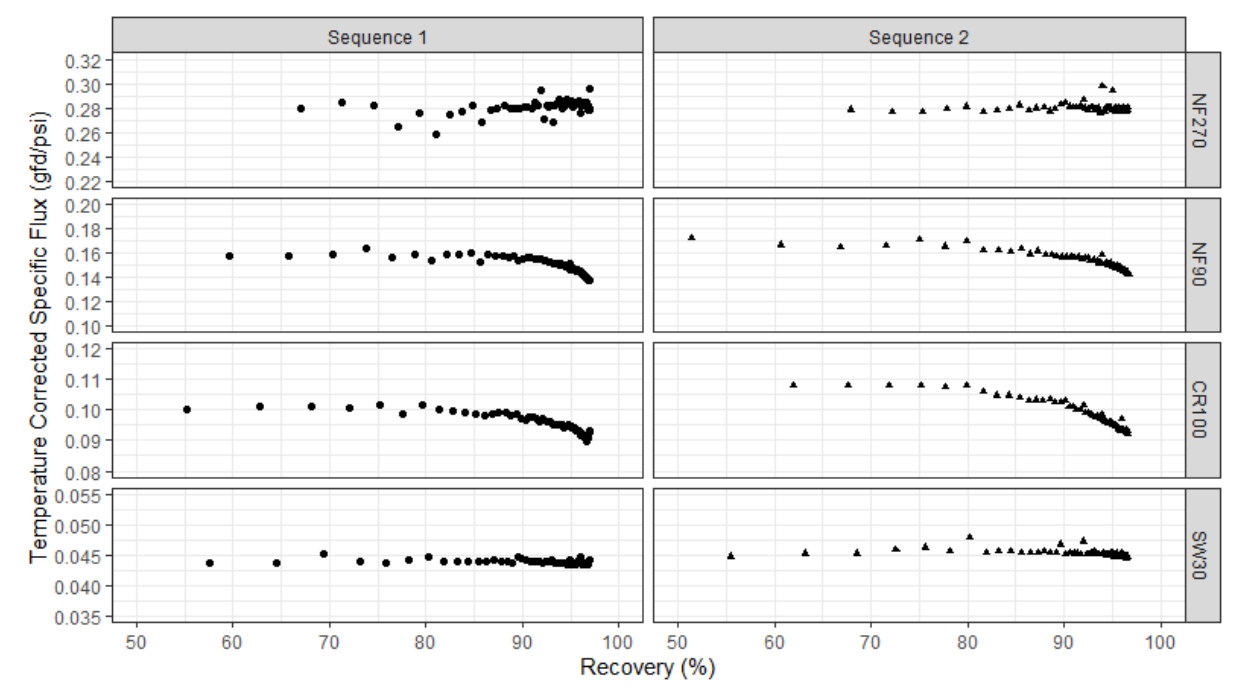


Figure 2. Candidate membrane TCSF as a function of recovery for two closed-circuit sequences.

Table 6. Specific Energy and Average TCSF for each 97% recovery membrane experiment

Membrane	Specific Energy (kWh/m³)	Average TCSF ^a (gfd/psi)
NF270	0.14	0.28
NF90	0.18	0.15
CR100	0.33	0.10
SW30	0.57	0.04

a. average TCSF presented as the arithmetic mean of n=126 TCSF calculations made at approximate 1 minute during the two sequence, 97% recovery experiments for each membrane.

3.1.2. PFAA rejection performance

A summary of the quantified feed solution (n=6) and final permeate (n=2) PFAA concentrations measured in the combined permeate tank and resulting calculated overall rejection values are presented in Figure 3. An additional method of estimating combined permeate concentrations by using PFAA permeate concentrations measured at discrete recovery values was also employed (Figures S.2 and S.3) and corroborated measured combined permeate concentrations presented in Figure 3. Of the membranes evaluated, the NF90, CR100, and SW30 achieved greater than 98.3% rejection of PFAAs after two sequences to 97% water recovery regardless of chain length or molecular weight. All PFAA feed concentrations were reduced to less than 100 ng/L in the combined permeate tank with PFOA and PFOS at or below the previous USEPA health advisory level (HAL) of 70 ng/L. These findings agreed with past studies reporting that the anionic nature of PFAAs and relatively large molecular weights compared to the MWCO of tight NF and RO membranes facilitates high separation.

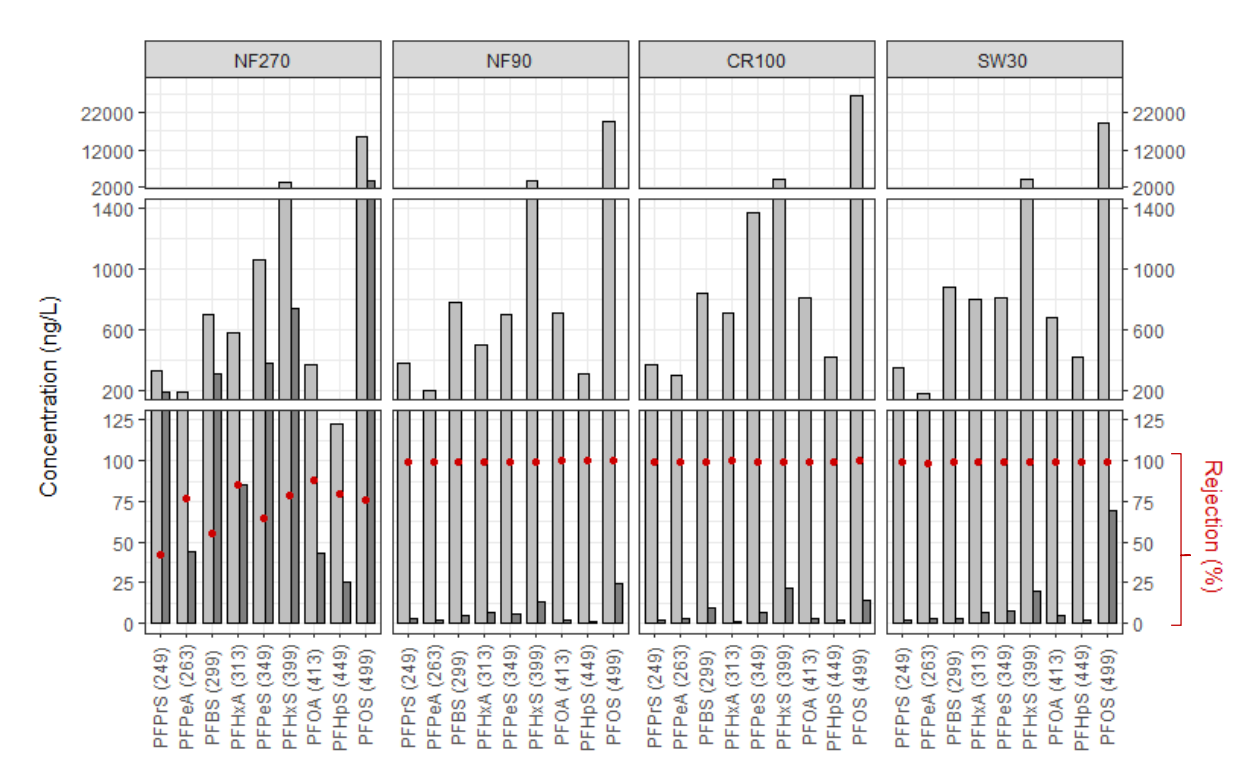


Figure 3. Feed (light grey) and permeate tank (dark grey) PFAA concentrations measured over two closed-circuit sequences and corresponding overall observed rejection values for candidate membranes. Molecular weight of PFAAs in parentheses. LOQ was used for calculating the average PFAA concentration when target PFAAs were not detected above their respective LOQ. Overall rejection values also presented in Table S.5.

Somewhat surprisingly, the loose NF membrane (NF270) displayed significantly higher permeate concentrations than the other candidate membranes resulting in PFAA rejection values ranging from 41.9 % (PFPrS) to 88.4 % (PFOA). This finding is somewhat contradictory to published literature that has highlighted the advantages of using loose NF for PFAA removal particularly, low pressure and energy requirements (Table 6), and partial passage of monovalent ions [23, 24, 48]. Several studies [22, 23, 27] have indicated that PFAA rejection by loose NF may be negatively impacted by increased ionic strength which also occurs at high recovery operation of CCMF systems. A substantial decline in observed and intrinsic rejection of certain PFAAs by the NF270 was measured above 90% recovery (see Section 3.2) however, this trend was not observed for TOC and was only marginally apparent for sulfate (Figure S.4). Additional tests were performed to investigate the impact of ionic strength on PFAA rejection (Section 3.3). Furthermore, the NF270 achieved higher rejections of PFCAs compared to PFSAs of greater molecular weight. For example, the final rejection of PFPeA (76.8%; MW: 263 g/mol) > PFBS

(55.4%; MW: 299 g/mol) and PFOA (88.4%; MW: 413 g/mol) > PFHpS (79.5%; MW: 449 g/mol). Interestingly, the observed rejection of PFOA by the NF270 exceeded that of PFOS, despite PFOS having a larger molecular volume. This observation suggests that PFAA headgroup might impact the rejection performance of PFAAs to a greater extent than molecular weight alone, particularly for the loose NF. Comparing the PFAA rejection results presented in Figure 3 and the specific energy presented in Table 5 for each membrane, the CR100 and SW30 membrane experiments required 1.8 and 3.2 times more energy than the NF90 to produce comparable PFAA permeate concentrations, respectively.

3.2. Impact of recovery on PFAA rejection performance

During CCMF operation in the absence of concentration polarization effects (e.g., electrostatic, adsorptive impacts), diffusive solute flux is anticipated to proportionally increase with system recovery [60]. Under this assumption, normalized intrinsic rejection is expected to remain constant and observed rejection is expected to decrease as recovery increases. Retentate and permeate samples collected during each CCMF sequence were used to determine the impact of recovery on intrinsic and observed rejection. The behavior of two representative long-chain PFAAs (PFOS and PFOA, Figure 4) and short-chain PFAAs (PFBS and PFPeA, Figure 5) are discussed below. Rejection versus recovery data for the remaining PFAAs quantified in this study are summarized in Figures S.4 and S.5.

The NF90, CR100, and SW30 membrane elements maintained >99.0% intrinsic rejection of all PFAAs up to 97% water recovery and were generally resistant to diminished long chain PFAA observed rejection performance at high recoveries (Figure 4 and Figured S.5 and S.6). However, the CR100's PFOA observed rejection performance began to decline at recoveries >94%, culminating in a net average decrease of approximately 0.6%. As noted above (Figure 3), PFAA rejection by the NF270 membrane elements were substantially lower than that observed for the NF90, CR100, and SW30 membrane elements. Additionally, the observed rejection of PFOA was negatively impacted by recovery (decrease of ~15%), likely due to increased feed-retentate solute concentration. However, during the NF270 experiment, observed PFOS rejection exhibited a relatively stable trend, with intrinsic rejection observed to increase with increasing recovery; Wang et al. [27] also reported increased PFOS rejection with increasing concentration. It is prudent to note that PFOS concentrations were two orders of magnitude greater than PFOA

in the feed water (Table 5), possibly impacting the intermolecular behavior of the compounds (e.g., self-assembly). These observations suggest that the predominant rejection mechanisms of the NF270 may be impacted by factors related to high recovery operation like increasing solute concentration or increasing ionic strength on the feed-retentate side of the membrane which are discussed in the next section.

PFBS and PFPeA rejection aligned more with traditional dilute solute behavior as a function of recovery with observed rejection decreasing for both solutes, although more significantly for PFBS. Similar to the long chain PFAA rejection performance comparison, the NF270 membrane elements were outperformed by the NF90, CR100, and SW30 membrane elements in rejecting short chain PFAAs at high recovery. At 97% water recovery the average observed rejection of PFBS and PFPeA by the NF270 was approximately 57% and 30%, respectively. The NF90, CR100, and SW30 maintained observed PFBS and PFPeA rejections >98.8% at 97% recovery. The SW30 membrane elements exhibited the best short chain PFAA rejection at high recovery, followed by the NF90 which maintained high selectivity for separation of PFPeA.

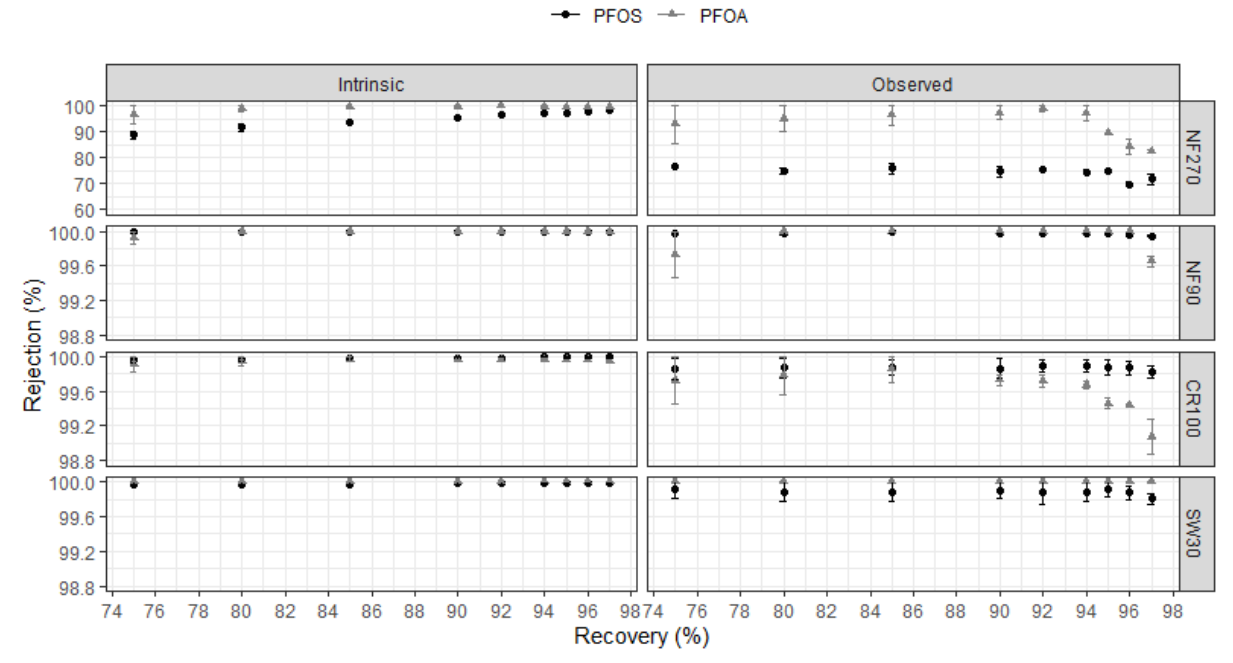


Figure 4. Rejection of PFOS and PFOA as a function of recovery for the four membrane elements evaluated. Note that y-axis scale changes depending on membrane element. Error bars represent deviation from average rejection values determined from the two closed-circuit sequences.

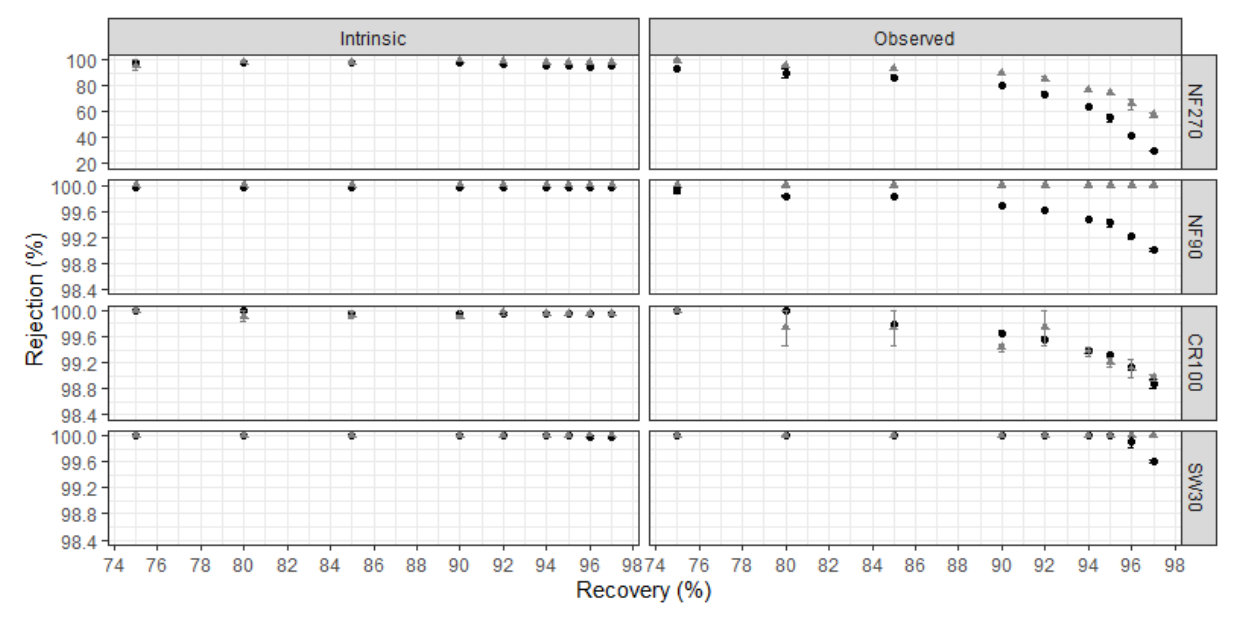


Figure 5. Rejection of PFBS and PFPeA as a function of recovery for the four membrane elementss evaluated. Note that y-axis scale changes depending on membrane element. Error bars represent deviation from average rejection values determined from the two closed-circuit sequences.

3.3. Impact of PFAA concentration and solution ionic strength on loose NF

Several unexpected trends were observed for PFAA separation performance by the NF270 membrane elements, including non-size dependent rejection of PFSAs (Figure 3), marked decrease of rejection for certain PFAAs at high recovery (Figures 4 and 5), and increasing PFOS rejection with increasing recovery (Figure 4). As noted in previous sections and in previous studies, both PFAA concentration (Wang et al. [27]) and feed water ion composition (Liu et al. [23]) are hypothesized to impact separation performance of certain membranes, particularly loose NF whose mechanisms for separation are both steric and electrostatic.

Concentration-dependent behavior might provide an explanation for the divergent intrinsic rejection trends observed for PFOS (increasing) and PFBS (decreasing) as a function of recovery (Figure 6, bottom pane). Although the critical micelle concentration (CMC) of PFOS has been reported between 698 and 5,000 mg/L, it has been demonstrated that some degree of self-aggregation can occur at concentrations in the fractional range of 0.001 and 0.01 of the CMC [61-64]. At approximately 90% recovery, the average feed-retentate PFOS concentration was measured at approximately 0.132 mg/L and at 97% recovery approximately 0.382 mg/L,

significantly lower than the reported CMCs (Figure 6). However, the CMC of a given PFAA can be a function of several parameters, including solution pH, PFAA chain length, and PFAA counter ions. Additionally, concentration polarization at the membrane surface driven, in part, by the increased hydrophobicity and lower charge density of the PFOS molecule may have increased the PFOS concentration near the membrane surface, above the measured bulk solution concentrations. It is possible that amphiphilic properties promoted the self-aggregation of PFOS, potentially resulting in increased supramolecular size (via aggregation) or the formation of a PFOS "gel" phase at the membrane surface.

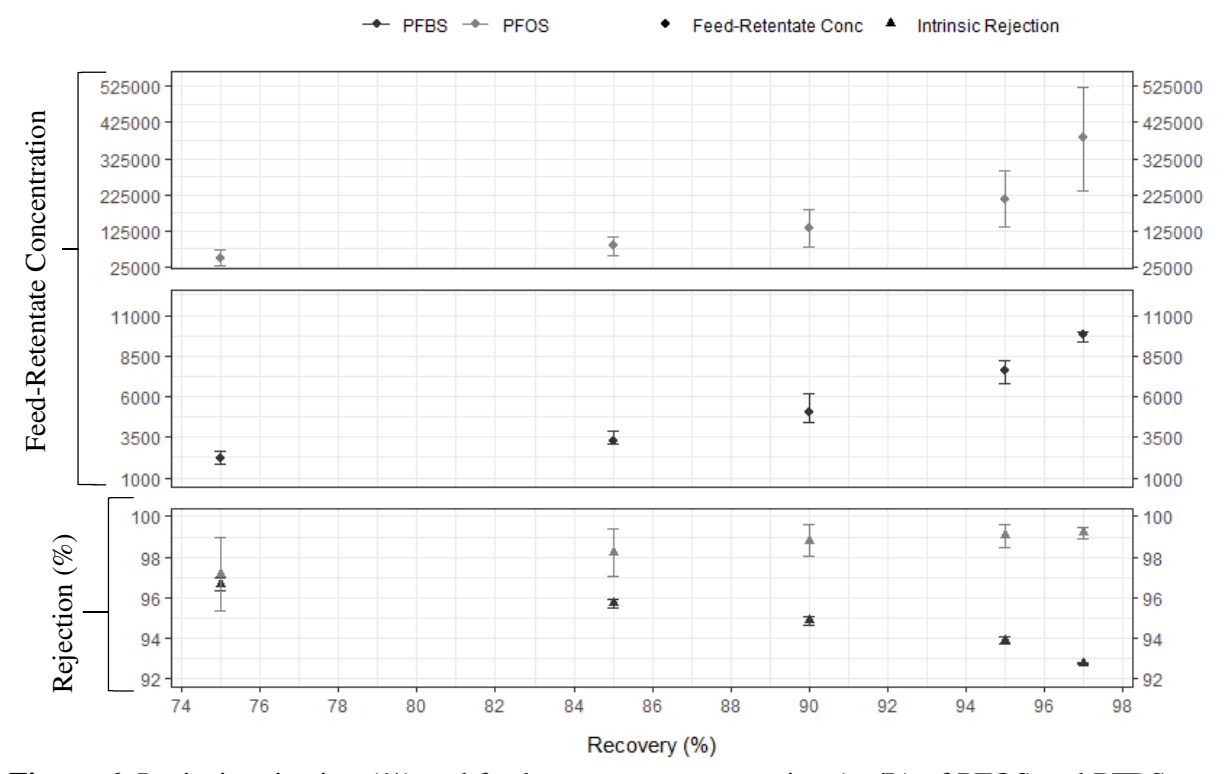


Figure 6. Intrinsic rejection (%) and feed-retentate concentration (ng/L) of PFOS and PFBS as a function of recovery. Data presented in Figure 6 incorporates a duplicate experiment and error bars are deviation from average values calculated from duplicate experiments. The feed water PFAA concentrations for the duplicate experiment are presented in Table S.6.

Previous studies have reported that the nominal molecular weight cut-off (MWCO) of the NF270 membrane elements is between 200 g/mol and 340 g/mol [54, 55]. The anionic molecular weights of PFBS and PFOS are approximately 299 g/mol and 499 g/mol, respectively (Table 1). Comparing the reported MWCO values of NF270 and the anionic molecular weights of PFBS and PFOS suggests that size exclusion could be the primary rejection mechanism of these solutes

by NF270. However, previous studies have demonstrated that electrostatic repulsion also plays a significant role in the rejection performance of anionic solutes by NF270 [28, 32, 35, 53].

To further investigate the role of electrostatic exclusion in PFBS and PFOS rejection by the NF270 membrane element, 500 grams of sodium sulfate (Na₂SO₄) were introduced into the feedwater. The 500-gram supplement of sodium sulfate represented the addition of approximately 0.85 mM of sulfate ion concentration and approximately 1.7 mM of sulfate ionic strength. Sulfate salt was selected for addition to the feedwater because it is a large divalent coion to the PFAA anions. Sulfate is typically well-rejected by the NF270 membrane and is expected to accumulate on the feed-retentate side of the system during CCMF operation. The addition of both ionic strength and a PFAA co-ion is expected to have a two-fold effect. The addition of ionic strength is expected to increase PFAA flux by reducing the time require to sufficiently suppress the repulsive electrostatic forces between the negatively charged membrane surface and the PFAA anions. Second, the high retention of a large divalent PFAA co-ion on the feed-retentate side of the membrane might induce increased Donnan-mediated migration of more mobile, shorter chain PFAAs across the membrane. On average, conductivity rejection during sulfate-amended experiments was higher than during baseline experiments presumably due to sulfate being a large divalent co-ion (Figures S.7 and S.8). Comparing the intrinsic rejection trends of PFBS and PFOS as a function of recovery between the baseline experiment and the sulfate-amended experiment it is apparent that the addition of sodium sulfate negatively impacted the rejection of PFBS and PFOS by the NF270 (Figure 7). Compared to the baseline experiment, the average intrinsic rejection decreased by 25.8% for PFBS and by 13.9% for PFOS at 97% water recovery during the sodium sulfate amended experiment. Wang et al. [27] reported a substantial decrease in PFBS rejection and a small increase in PFOS rejection upon addition of 10 to 100 mM sodium chloride by an NF membrane of similar material (poly-piperazine). These changes were attributed to reduced electrostatic repulsion (PFBS) and enhanced steric exclusion (PFOS) at the higher ionic strengths investigated. While it can be hypothesized that the addition of a divalent co-ion (sulfate) in this work and higher recoveries evaluated had a more significant impact on PFOS rejection compared to findings of Wang et al., [27], additional controlled studies are necessary to elucidate the mechanisms responsible.



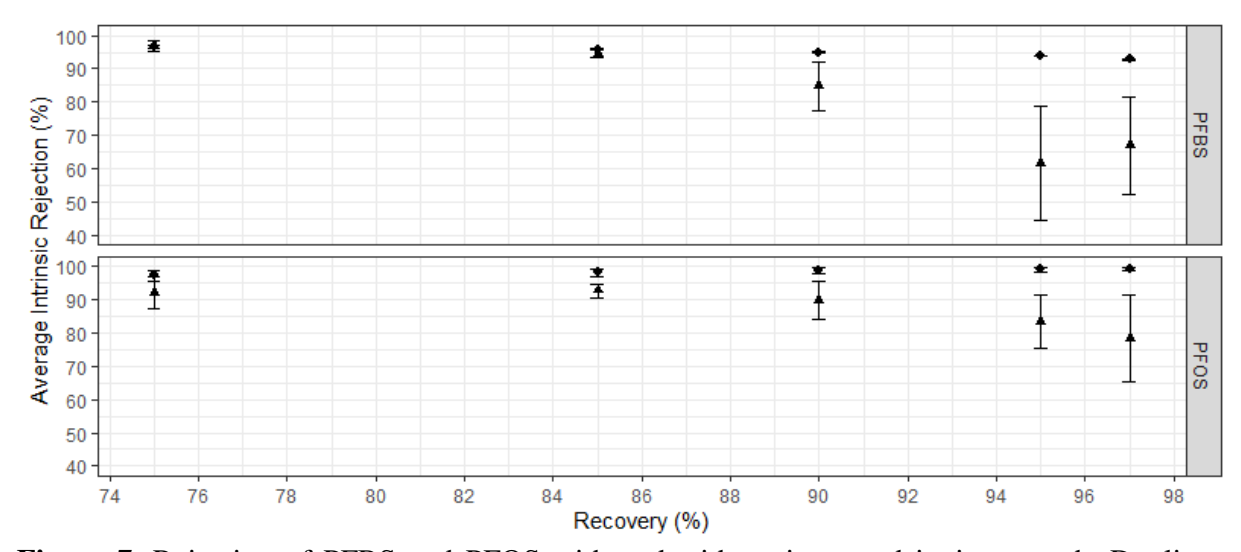


Figure 7. Rejection of PFBS and PFOS with and without increased ionic strength. Duplicate baseline experiment is black circles and sodium sulfate experiment is black triangle. Error bars represent deviation from average rejection values determined from the two closed-circuit sequences.

4. Conclusion

The present study investigated the PFAA rejection performance of four commercial high-pressure membranes spanning characteristics of loose NF to tight RO in a pilot-scale CCMF system operating up to 97% water recovery. The loose NF investigated (NF270) exhibited the lowest PFAA rejection performance during the high recovery experiments, particularly at water recoveries >90%. The diminished PFAA rejection performance of the NF270 at water recoveries >90% is likely a result of both steric and electrostatic exclusion being significant separation mechanisms. During CCMF operation, because ionic strength increases on the feed-retentate side of the membrane, repulsive electrostatic forces are hypothesized to diminish, leading to increased PFAS permeation with increasing water recovery. Feed water amended with sodium sulfate yielded lower rejection for PFAAs by the NF270 compared to unamended feed water supporting the hypothesis that high recovery CCMF operation may negatively impact PFAS rejection by loose NF membranes, particularly membranes that rely on electrostatic exclusion for separation of anions.

The results of this study demonstrate that tight NF and RO membranes are effective for separating and concentrating PFAAs during high recovery CCMF operation. During CCMF

sequences to 97% water recovery, the NF90, CR100, and SW30 membranes exhibited overall rejection values of >98.3% for the PFAAs quantified in this study. Measured intrinsic PFAA rejection values for these three membranes exceeded 99% (greater than 99.9% was measured for certain PFAAs) throughout 97% water recovery CCMF sequences. Effective PFAS concentration and residual volume reduction are critical to cost-effective implementation of selective PFAS treatment, particularly emergent destructive technologies. The demonstrated effectiveness of tight NF membranes in highly rejecting PFAAs at high recoveries while exhibiting relatively low specific energy is of particular interest.

Future study should focus on specific components of long-term high recovery CCMF operation, including potential impacts on PFAS rejection, membrane fouling, and life cycle costs. Additionally, the development of a membrane optimized for PFAS selectivity and fouling mitigation at high recoveries may be of significant value in PFAS specific treatment applications.

Acknowledgements

The authors would like to thank Nathan Rothe (Colorado School of Mines) for helping with sample preparation and analysis and Michael Veres (Colorado School of Mines) for his help with system integration and technical support. We thank FilmTecTM for providing membrane elements for testing, and Desalitech Inc for technical support and use of a pilot-scale DesaliTecTM CCMF system. This research was funded by the U.S. Department of Defense Environmental Security Technology Certification Program (ESTCP) under project ER18-5053 and ER20-5369. The comments and views detailed herein may not necessarily reflect the views of ESTCP, its officers, directors, affiliates, or agents.

References

[1] Z. Wang, J.C. DeWitt, C.P. Higgins, I.T. Cousins, A Never-Ending Story of Per- and Polyfluoroalkyl Substances (PFASs)?, Environmental Science & Technology, 51 (2017) 2508-2518.

[2] K.J. Hansen, L.A. Clemen, M.E. Ellefson, H.O. Johnson, Compound-Specific, Quantitative Characterization of Organic Fluorochemicals in Biological Matrices, Environmental Science & Technology, 35 (2001) 766-770.

[3] M.S. Kirk, K.; Braunig, J.; Trevenar, S.; D'Este, C.; Lucas, R.; Lal, A.; Korda, R.; Clements, A.; Mueller, J.; Armstrong, B., The PFAS Health Study: Systematic Literature Review, in, Australian National University, 2018.

- [4] The Interstate Technology & Regulatory Council (ITRC) Per- and Polyfluoroalkyl Substances (PFAS) Team, Technical/Regulatory Guidance: Per- and Polyfluoroalkyl Substances (PFAS), in, 2020.
- [5] F. Pontius, Regulation of Perfluorooctanoic Acid (PFOA) and Perfluorooctane Sulfonic Acid (PFOS) in Drinking Water: A Comprehensive Review, in: Water, 2019.
- [6] USEPA, Lifetime health advisories and health effects support documents for perfluorooctanoic acid and perfluorooctane sulfonate., in, Office of Pesticide Programs, 2016.
- [7] USEPA, Drinking Water Health Advisories for PFOA and PFOS; 2022 Interim Updated PFOA and PFOS Health Advisories, in, 2022.
- [8] United States Environmental Protection Agency, Proposed PFAS National Primary Drinking Water Regulation, in, 2023.
- [9] T.D. Appleman, C.P. Higgins, O. Quiñones, B.J. Vanderford, C. Kolstad, J.C. Zeigler-Holady, E.R.V. Dickenson, Treatment of poly- and perfluoroalkyl substances in U.S. full-scale water treatment systems, Water Research, 51 (2014) 246-255.
- [10] P. McCleaf, S. Englund, A. Östlund, K. Lindegren, K. Wiberg, L. Ahrens, Removal efficiency of multiple poly- and perfluoroalkyl substances (PFASs) in drinking water using granular activated carbon (GAC) and anion exchange (AE) column tests, Water Research, 120 (2017) 77-87.
- [11] N. Merino, Q. Yan, R.A. Deeb, E.L. Hawley, M.R. Hoffmann, S. Mahendra, Degradation and removal methods for perfluoroalkyl and polyfluoroalkyl substances in water, Environmental Engineering Science, 33 (2016) 615-649.
- [12] R.K. Singh, N. Multari, C. Nau-Hix, R.H. Anderson, S.D. Richardson, T.M. Holsen, S. Mededovic Thagard, Rapid Removal of Poly- and Perfluorinated Compounds from Investigation-Derived Waste (IDW) in a Pilot-Scale Plasma Reactor, Environmental Science & Technology, 53 (2019) 11375-11382.
- [13] R. Tenorio, J. Liu, X. Xiao, A. Maizel, C.P. Higgins, C.E. Schaefer, T.J. Strathmann, Destruction of Per- and Polyfluoroalkyl Substances (PFASs) in Aqueous Film-Forming Foam (AFFF) with UV-Sulfite Photoreductive Treatment, Environmental Science & Technology, 54 (2020) 6957-6967.
- [14] S. Hao, Y.-J. Choi, B. Wu, C.P. Higgins, R. Deeb, T.J. Strathmann, Hydrothermal Alkaline Treatment for Destruction of Per- and Polyfluoroalkyl Substances in Aqueous Film-Forming Foam, Environmental Science & Technology, 55 (2021) 3283-3295.
- [15] B.R. Pinkard, S. Shetty, D. Stritzinger, C. Bellona, I.V. Novosselov, Destruction of perfluorooctanesulfonate (PFOS) in a batch supercritical water oxidation reactor, Chemosphere, 279 (2021) 130834.
- [16] A. Soriano, C. Schaefer, A. Urtiaga, Enhanced treatment of perfluoroalkyl acids in groundwater by membrane separation and electrochemical oxidation, Chemical Engineering Journal Advances, 4 (2020) 100042.
- [17] G.R. Stratton, F. Dai, C.L. Bellona, T.M. Holsen, E.R.V. Dickenson, S. Mededovic Thagard, Plasma-based water treatment: Efficient transformation of perfluoroalkyl substances (PFASs) in prepared solutions and contaminated groundwater, Environmental Science & Technology, (2017).

- [18] C.C. Murray, R.E. Marshall, C.J. Liu, H. Vatankhah, C.L. Bellona, PFAS treatment with granular activated carbon and ion exchange resin: Comparing chain length, empty bed contact time, and cost, Journal of Water Process Engineering, 44 (2021) 102342.
- [19] C. Liu, D. Werner, C. Bellona, Removal of per- and polyfluoroalkyl substances (PFASs) from contaminated groundwater using granular activated carbon: a pilot-scale study with breakthrough modeling Environmental Science: Water Research and Technology, Advance Article (2019).
- [20] T.H. Boyer, Y. Fang, A. Ellis, R. Dietz, Y.J. Choi, C.E. Schaefer, C.P. Higgins, T.J. Strathmann, Anion exchange resin removal of per- and polyfluoroalkyl substances (PFAS) from impacted water: A critical review, Water Research, 200 (2021) 117244.
- [21] C. Bellona, J.E. Drewes, G. Oelker, J. Luna, G. Filteau, G. Amy, Comparing nanofiltration and reverse osmosis for drinking water augmentation, Journal of the American Waterworks Association, 100 (2008) 102-116.
- [22] E. Steinle-Darling, M. Reinhard, Nanofiltration for Trace Organic Contaminant Removal: Structure, Solution, and Membrane Fouling Effects on the Rejection of Perfluorochemicals, Environmental Science & Technology, 42 (2008) 5292-5297.
- [23] C.J. Liu, T.J. Strathmann, C. Bellona, Rejection of per- and polyfluoroalkyl substances (PFASs) in aqueous film-forming foam by high-pressure membranes, Water Research, 188 (2021) 116546.
- [24] T.D. Appleman, E.R.V. Dickenson, C. Bellona, C.P. Higgins, Nanofiltration and granular activated carbon treatment of perfluoroalkyl acids, Journal of Hazardous Materials, 260 (2013) 740-746.
- [25] C.Y. Tang, Q.S. Fu, C.S. Criddle, J.O. Leckie, Effect of Flux (Transmembrane Pressure) and Membrane Properties on Fouling and Rejection of Reverse Osmosis and Nanofiltration Membranes Treating Perfluorooctane Sulfonate Containing Wastewater, Environmental Science & Technology, 41 (2007) 2008-2014.
- [26] C.Y. Tang, Q.S. Fu, A.P. Robertson, C.S. Criddle, J.O. Leckie, Use of Reverse Osmosis Membranes to Remove Perfluorooctane Sulfonate (PFOS) from Semiconductor Wastewater, Environmental Science & Technology, 40 (2006) 7343-7349.
- [27] J. Wang, L. Wang, C. Xu, R. Zhi, R. Miao, T. Liang, X. Yue, Y. Lv, T. Liu, Perfluorooctane sulfonate and perfluorobutane sulfonate removal from water by nanofiltration membrane: The roles of solute concentration, ionic strength, and macromolecular organic foulants, Chemical Engineering Journal, 332 (2018) 787-797.
- [28] C. Bellona, J.E. Drewes, P. Xu, G. Amy, Factors affecting the rejection of organic solutes during NF/RO treatment—a literature review, Water Research, 38 (2004) 2795-2809.
- [29] K.O. Agenson, J.-I. Oh, T. Urase, Retention of a wide variety of organic pollutants by different nanofiltration/reverse osmosis membranes: controlling parameters of process, Journal of Membrane Science, 225 (2003) 91-103.
- [30] H.Q. Dang, L.D. Nghiem, W.E. Price, Factors governing the rejection of trace organic contaminants by nanofiltration and reverse osmosis membranes, Desalination and Water Treatment, 52 (2014) 589-599.

- [31] Y. Kiso, Y. Sugiura, T. Kitao, K. Nishimura, Effects of hydrophobicity and molecular size on rejection of aromatic pesticides with nanofiltration membranes, Journal of Membrane Science, 192 (2001) 1-10.
- [32] C. Bellona, J.E. Drewes, The role of membrane surface charge and solute physico-chemical properties in the rejection of organic acids by NF membranes, Journal of Membrane Science, 249 (2005) 227-234.
- [33] A.M. Comerton, R.C. Andrews, D.M. Bagley, P. Yang, Membrane adsorption of endocrine disrupting compounds and pharmaceutically active compounds, Journal of Membrane Science, 303 (2007) 267-277.
- [34] A.R.D. Verliefde, E.R. Cornelissen, S.G.J. Heijman, J.Q.J.C. Verberk, G.L. Amy, B. Van der Bruggen, J.C. van Dijk, The role of electrostatic interactions on the rejection of organic solutes in aqueous solutions with nanofiltration, Journal of Membrane Science, 322 (2008) 52-66.
- [35] H. Ozaki, H. Li, Rejection of organic compounds by ultra-low pressure reverse osmosis membrane, Water Research, 36 (2002) 123-130.
- [36] K. Kimura, G. Amy, J.E. Drewes, T. Heberer, T.-U. Kim, Y. Watanabe, Rejection of organic micropollutants (disinfection by-products, endocrine disrupting compounds, and pharmaceutically active compounds) by NF/RO membranes, Journal of Membrane Science, 227 (2003) 113-121.
- [37] T.F. Mastropietro, R. Bruno, E. Pardo, D. Armentano, Reverse osmosis and nanofiltration membranes for highly efficient PFASs removal: overview, challenges and future perspectives, Dalton Transactions, 50 (2021) 5398-5410.
- [38] X. Hang, X. Chen, J. Luo, W. Cao, Y. Wan, Removal and recovery of perfluorooctanoate from wastewater by nanofiltration, Separation and Purification Technology, 145 (2015) 120-129.
- [39] L.F. Greenlee, D.F. Lawler, B.D. Freeman, B. Marrot, P. Moulin, Reverse osmosis desalination: Water sources, technology, and today's challenges, Water Research, 43 (2009) 2317-2348.
- [40] A. Shahmansouri, J. Min, L. Jin, C. Bellona, Feasibility of extracting valuable minerals from desalination concentrate: a comprehensive literature review, Journal of Cleaner Production, 100 (2015) 4-16.
- [41] A. Efraty, R.N. Barak, Z. Gal, Closed circuit desalination series no-2: new affordable technology for sea water desalination of low energy and high flux using short modules without need of energy recovery, Desalination and Water Treatment, 42 (2012) 189-196.
- [42] A. Efraty, R.N. Barak, Z. Gal, Closed circuit desalination A new low energy high recovery technology without energy recovery, Desalination and Water Treatment, 31 (2011) 95-101.
- [43] R.L. Stover, Industrial and brackish water treatment with closed circuit reverse osmosis, Desalination and Water Treatment, 51 (2013) 1124-1130.
- [44] S. Lin, M. Elimelech, Staged reverse osmosis operation: Configurations, energy efficiency, and application potential, Desalination, 366 (2015) 9-14.

- [45] S. Lin, M. Elimelech, Kinetics and energetics trade-off in reverse osmosis desalination with different configurations, Desalination, 401 (2017) 42-52.
- [46] D.M. Warsinger, E.W. Tow, K.G. Nayar, L.A. Maswadeh, J.H. Lienhard V, Energy efficiency of batch and semi-batch (CCRO) reverse osmosis desalination, Water Research, 106 (2016) 272-282.
- [47] D.M. Warsinger, E.W. Tow, L.A. Maswadeh, G.B. Connors, J. Swaminathan, J.H. Lienhard V, Inorganic fouling mitigation by salinity cycling in batch reverse osmosis, Water Research, 137 (2018) 384-394.
- [48] C.J. Liu, G. McKay, D. Jiang, R. Tenorio, J.T. Cath, C. Amador, C.C. Murray, J.B. Brown, H.B. Wright, C. Schaefer, C.P. Higgins, C. Bellona, T.J. Strathmann, Pilot-scale field demonstration of a hybrid nanofiltration and UV-sulfite treatment train for groundwater contaminated by per- and polyfluoroalkyl substances (PFASs), Water Research, 205 (2021) 117677.
- [49] J.F. Fernández, B. Jastorff, R. Störmann, S. Stolte, J. Thöming, Thinking in Terms of Structure-Activity-Relationships (T-SAR): A Tool to Better Understand Nanofiltration Membranes, Membranes (Basel), 1 (2011) 162-183.
- [50] K.L. Tu, L.D. Nghiem, A.R. Chivas, Coupling effects of feed solution pH and ionic strength on the rejection of boron by NF/RO membranes, Chemical Engineering Journal, 168 (2011) 700-706.
- [51] Y.-N. Kwon, K. Shih, C. Tang, J.O. Leckie, Adsorption of perfluorinated compounds on thin-film composite polyamide membranes, Journal of Applied Polymer Science, 124 (2012) 1042-1049.
- [52] L.D. Nghiem, A.I. Schäfer, M. Elimelech, Removal of Natural Hormones by Nanofiltration Membranes: Measurement, Modeling, and Mechanisms, Environmental Science & Technology, 38 (2004) 1888-1896.
- [53] C. Boo, Y. Wang, I. Zucker, Y. Choo, C.O. Osuji, M. Elimelech, High Performance Nanofiltration Membrane for Effective Removal of Perfluoroalkyl Substances at High Water Recovery, Environmental Science & Technology, 52 (2018) 7279-7288.
- [54] M.J. López-Muñoz, A. Sotto, J.M. Arsuaga, B. Van der Bruggen, Influence of membrane, solute and solution properties on the retention of phenolic compounds in aqueous solution by nanofiltration membranes, Separation and Purification Technology, 66 (2009) 194-201.
- [55] L. Braeken, B. Bettens, K. Boussu, P. Van der Meeren, J. Cocquyt, J. Vermant, B. Van der Bruggen, Transport mechanisms of dissolved organic compounds in aqueous solution during nanofiltration, Journal of Membrane Science, 279 (2006) 311-319.
- [56] H.M. Krieg, S.J. Modise, K. Keizer, H.W.J.P. Neomagus, Salt rejection in nanofiltration for single and binary salt mixtures in view of sulphate removal, Desalination, 171 (2005) 205-215.
- [57] K.L. Tu, A.r. Chivas, L.D. Nghiem, Effects of membrane fouling and scaling on boron rejection by nanofiltration and reverse osmosis membranes, Desalination, 279 (2011) 269-277.
- [58] L. Zhu, Rejection of Organic Micropollutants by Clean and Fouled Nanofiltration Membranes, Journal of Chemistry, 2015 (2015) 934318.

- [59] J.T. Arena, B. McCloskey, B.D. Freeman, J.R. McCutcheon, Surface modification of thin film composite membrane support layers with polydopamine: Enabling use of reverse osmosis membranes in pressure retarded osmosis, Journal of Membrane Science, 375 (2011) 55-62.
- [60] R.I. Urama, B.J. Mariñas, Mechanistic interpretation of solute permeation through a fully aromatic polyamide reverse osmosis membrane, Journal of Membrane Science, 123 (1997) 267-280.
- [61] Q. Yu, R. Zhang, S. Deng, J. Huang, G. Yu, Sorption of perfluorooctane sulfonate and perfluorooctanoate on activated carbons and resin: Kinetic and isotherm study, Water Research, 43 (2009) 1150-1158.
- [62] K. Shih, F. Wang, Adsorption Behavior of Perfluorochemicals (PFCs) on Boehmite: Influence of Solution Chemistry, Procedia Environmental Sciences, 18 (2013) 106-113.
- [63] R.L. Johnson, A.J. Anschutz, J.M. Smolen, M.F. Simcik, R.L. Penn, The Adsorption of Perfluorooctane Sulfonate onto Sand, Clay, and Iron Oxide Surfaces, Journal of Chemical & Engineering Data, 52 (2007) 1165-1170.
- [64] J. Costanza, M. Arshadi, L.M. Abriola, K.D. Pennell, Accumulation of PFOA and PFOS at the Air–Water Interface, Environmental Science & Technology Letters, 6 (2019) 487-491.

